Nuclear Ramsauer effect and the isovector potential

J. D. Anderson and S. M. Grimes*
Lawrence Livermore National Laboratory, University of California, Livermore, California 94550
(Received 23 August 1989)

The simple nuclear Ramsauer model is extended to include explicitly the isovector potential. This model predicts large differences between proton and neutron total nuclear cross sections. When this model is applied to isotope/isotone total neutron cross section differences, it gives a good description of the measured data in the mass 140 region. Non-isospin-dependent differences in the isotopic imaginary potential are observed which totally obscure the contribution from the isovector imaginary potential. Additional measurements further from closed nuclear shells may yield useful information on the isovector imaginary potential.

I. INTRODUCTION

Over 35 years ago Lawson[1] interpreted maxima and minima as a function of energy in total neutron cross sections in terms of a very simple model[2] and further examination of the details of this model has been carried out by Peterson[3] and McVoy.[4] Peterson used the term nuclear Ramsauer effect to describe a single "average" phase-shift approximation which had the same form as the well-known low-energy electron scattering interference phenomena known as the Ramsauer-Townsend effect.[5] The interference properties of the nuclear Ramsauer effect have been used recently by Gould *et al.*[6] to elucidate the differences between the real and imaginary parts of the two-body spin-dependent force. It was Gould's work[6] which motivated the extension of this simple model to include isospin.

We begin by briefly describing the nuclear Ramsauer model. We then apply it to the high-precision total cross-section data set of Camarda *et al.*[7] to assess the phenomenological utility of the model. We next explore a logical extension of the model to include isospin. The effect of the isovector potential on precision isotopic total cross section is then estimated and compared to experiment.

Before proceeding with our discussion it is important to note that optical-model calculations give a reasonable account of all the data presented here. The optical-model calculations generally involve many partial waves and are so complex that it is not easy to get a simple interpretation or intuitive picture of the basic processes involved in these interactions. It is our intent, in adding isospin to this simple Ramsauer model, to gain a more intuitive understanding of these processes. This model does not remove the need for doing optical-model calculations, but can be used effectively to guide choices of targets and energy regions of analysis for most efficient use of resources. We point out that certain energy regions for specific targets are much less useful than others in determining isovector optical potentials.

II. NUCLEAR RAMSAUER MODEL

The basic picture of the nuclear Ramsauer effect, as used by Peterson[3] to describe neutron total cross sections, is shown in Fig. 1. A neutron wave is incident on a nucleus represented by a potential well of radius R. Interference between that part of the wave which has traversed the nucleus and that part which has gone around causes oscillations in the total cross section.

To be more precise we write the usual scattering amplitude at zero degrees as

$$f(0^\circ)=\frac{i}{2k}\sum_{l=0}^{L}(2l+1)(1-e^{2in_l}) . \tag{1}$$

In our simple model of Fig. 1, if we take n_l independent of l we can easily sum over l to obtain

$$f(0^\circ)=ik(R+\lambda\!\!\!^{-})^2(1-\alpha e^{i\beta})/2 , \tag{2}$$

where we have replaced $e^{2i\eta}$ by $\alpha e^{i\beta}$ and where we have taken the maximum value of l to be $L=kR$. Since the total cross section is related to the imaginary part of the zero-degree scattering amplitude by

$$\sigma_T=\frac{4\pi}{k}\mathrm{Im}f(0^\circ) , \tag{3}$$

we obtain

$$\sigma_T=2\pi(R+\lambda\!\!\!^{-})^2(1-\alpha\cos\beta) . \tag{4}$$

The average behavior of the total cross section is described by $\sigma_T=2\pi(R+\lambda\!\!\!^{-})^2$ (the black nucleus approximation) and the effect of the coherent nuclear Ramsauer effect is reflected in the $(1-\alpha\cos\beta)$ term. The argument of the periodic term, β, can be understood in terms of the change in phase of a wave scattered at the nuclear surface and passing through a medium with an index of refraction, i.e.,

$$\beta\approx\tfrac{4}{3}nR(k_{\mathrm{in}}-k_{\mathrm{out}}) \tag{5}$$

when $\frac{4}{3}R$ is the average chord length of a neutron passing through the nucleus, n is an index of refraction, k_{out} is the wave number outside the nucleus, and k_{in} is the wave number inside the nucleus. The coefficient α represents the absorption of the incident wave and in this crude model is given by

$$\alpha=e^{-W\bar{R}\sqrt{2m}/\hbar\sqrt{E+V}} , \tag{6}$$

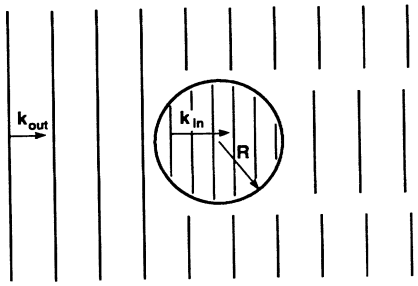

FIG. 1. Schematic representation of the Ramsauer process. A neutron wave is incident on the nucleus represented by a square-well potential of radius R. Interference between that part of the wave going through the nucleus and that part which has gone around causes oscillations in the neutron total cross section.

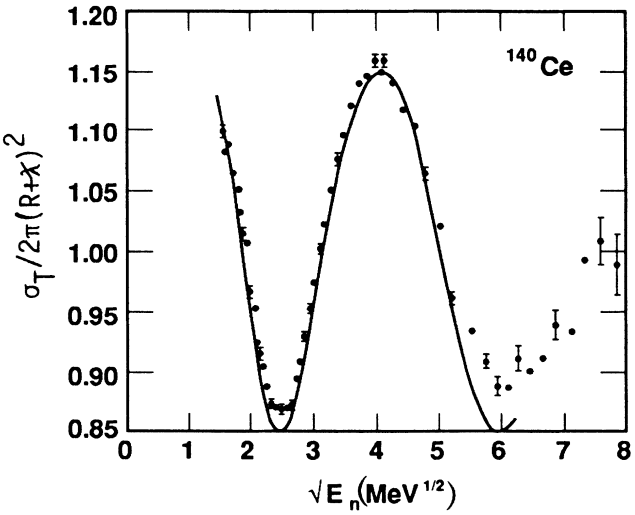

FIG. 2. The quantity $\sigma_T/2\pi(R+\lambda\!\!\!^{-})^2$ is plotted versus the square root of the neutron bombarding energy. R is taken from Ref. 3 as $1.35A^{1/3}$. The data are from Ref. 7. Our phenomenological fit is shown as the solid curve.

where W is the average absorption (imaginary) potential, $\bar{R}$ is an appropriate nuclear dimension, and V is the real potential.

At first glance our assumption that η_l is independent of l seems unrealistic. However, McVoy[8] found, via optical-model calculations, that the peak in the total neutron cross section was due to many partial waves passing downward through 90° at approximately the same neutron energy, i.e., at least at the peak of the total cross section several partial waves do have approximately the same phase. Secondly, if we assumed an amplitude dependence of α on l this would be subsumed in our empirical model by adding an additional energy dependence to α. Also, assuming the nucleus is "black" out to some arbitrary radius, and then applying our model, yields a renormalization of α but the form should still be correct. Thus, we conclude that although the assumptions used to derive our simple model are not well met, the empirical form of the total cross section is rather robust against reasonable variations in parameters.

III. FITTING TO PRECISION DATA

For ^{140}Ce, Camarda *et al.*[7] have measured the total neutron cross section over the energy range of 2–60 MeV with a relative error of between $\frac{1}{4}-\frac{1}{2}$% and with an absolute uncertainty of 1.5–2%. We first divide the measured cross sections by $2\pi(R+\lambda\!\!\!^{-})^2$, where R is taken from Peterson[3] as $1.35A^{1/3}$ fm. We then plot this normalized cross section versus $\sqrt{E}$ in Fig. 2. We choose $\sqrt{E}$ as the abscissa since this should be the primary variable causing the phase change β. From Fig. 2 we can quite accurately determine both the zero crossings and the peak positions. These are plotted in Fig. 3. The absolute value of β can be calculated approximately by Eq. (5) or absolutely by counting the number of maxima in Ref. 3. We then generate $\beta(\sqrt{E})$ via two linear least-squares fits jointed at $E_n=9.7$ MeV.[9] For comparison we also include a calculation of β using the normal energy dependence of the real optical potential taken from Camarda *et al.*[7] To make a realistic comparison between our fit to β and optical-model calculations, we would need to use an optical potential for which dispersion

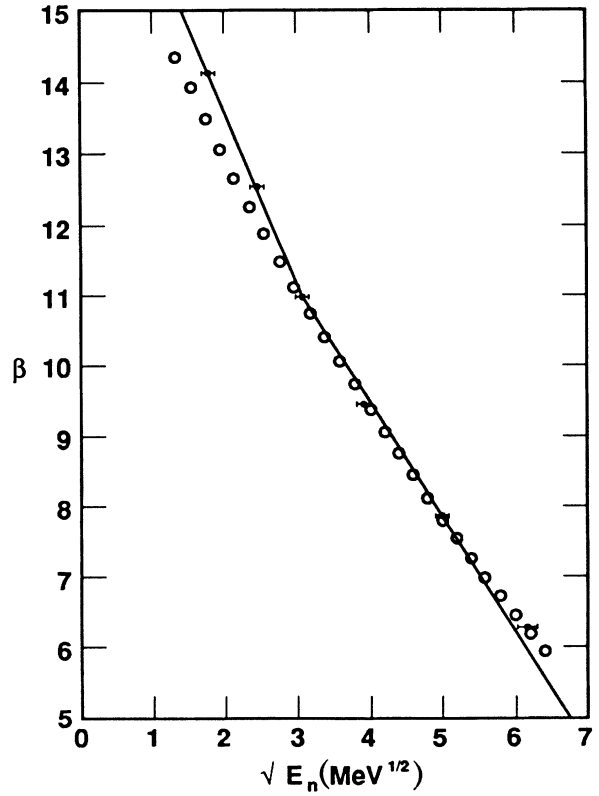

FIG. 3. The plotted values of β with their associated errors are determined from the location of zero crossings, maxima, and minima shown in Fig. 2. The solid lines are two first-order least-squares fits joined at $\beta=11.0$. The smooth curve is obtained from using a smooth optical potential derived from Ref. 7 and normalized at $\beta=11.0$.

corrections have been made, e.g., the Fermi surface anomaly.[10] Since such corrections are not available to us, we simply note that they are of the right sign and magnitude to account for the deviation between our fit and the optical-model calculations.

By inspection it appears $\alpha=0.15$ is a good approximation below $E_n \sim 25$ MeV. Our fit to the data is shown as a solid curve in Fig. 2. If we reduce the measured data by 1% (well within the absolute uncertainty of 1.5–2 %) or if we increase the radius by $\frac{1}{2}$%, the model fit to the data is excellent. At first glance it may seem obvious that a polynomial expansion (or any smooth function) for β would produce a good fit to the data. However, remembering that the actual cross section is a sum over contributions from many partial waves with different phases and with slightly different energy dependence it is not clear that even the form of Eq. (4) would be applicable at low energies. It is therefore somewhat surprising and perhaps fortuitous that this model gives such an excellent description of the neutron total cross section at such a high level of precision. Since our model is at least phenomenologically useful we proceed to extend the model to include isospin.

IV. EXTENSION TO INCLUDE ISOSPIN

In Gould *et al.*[6] the spin-spin (ss) cross section is defined as

$$\sigma_{ss}=(\sigma_p-\sigma_a)/2 , \tag{7}$$

where σ_p (σ_a) is the total neutron cross section for neutron and target spins parallel (antiparallel). In analogy to Ref. 4, we define an isospin-isospin cross section σ_{is} as

$$\sigma_{is}=(\sigma_T^{>}-\sigma_T^{<})/2 , \tag{8}$$

where $>$ and $<$ refer to isospin parallel ($T_0+\frac{1}{2}$) and antiparallel ($T_0-\frac{1}{2}$) projections. The $\sigma_T^{>}$ is our neutron total cross section and for large $(N-Z)$, $\sigma^{<}$ should be fairly accurately represented by the proton nuclear total cross section, i.e., excluding Coulomb scattering.

If we assume[6] that there are small changes in the real and imaginary optical potentials due to an isovector potential of the form $1/A \times \mathbf{t}\cdot\mathbf{T}(V_1+iW_1)$, then these small changes in the real and imaginary potentials yield out of phase contributions in the change in the total cross section. A measurement of σ_{is}, which is performed at an energy where a change in W has no effect on σ_{is}, is sensitive only to the real isovector potential and vice versa.

To show this explicitly we proceed as follows. Equation (4) can be written as

$$\sigma_T^{>}=2\pi(R+\lambda\!\!\!^{-})^2(1-\alpha^{>}\cos\beta^{>}) .$$

If we also assume V_1 and W_1 are small[11] compared to V and W so we can express $\beta^{>}=\beta^{<}(1+\epsilon)$, where ϵ is the change in β due to V_1 and likewise $\alpha^{>}=\alpha^{<}(1+\delta)$ where δ is a small change in absorption due to W_1, we obtain

$$\sigma_{is}=\pi(R+\lambda\!\!\!^{-})^2\alpha^{>}(-\delta\cos\beta^{>}+\epsilon\beta^{>}\sin\beta^{>}) . \tag{9}$$

Thus, we explicitly obtain the sensitivity we were looking for, i.e., the effect of the imaginary isovector potential varies as $\cos\beta$ while the effect due to the real part is contained in the coefficient of $\sin\beta$.

In order to illustrate the magnitude and energy dependence of our isospin transfer cross section σ_{is}, we use the Lane[12] form of the isospin dependent optical potential and normalize the potential values to the neutron parameters taken from Camarda *et al.*[7] Our potentials are given by

$$\begin{aligned} V^{>}&=V_0-\frac{N-Z}{4}\frac{V_1}{A}-0.3E^{>} , \\ V^{<}&=V_0+\frac{N-Z}{4}\frac{V_1}{A}-0.3E^{<} , \end{aligned} \tag{10}$$

where V_0 is the isospin independent potential, V_1 is our real isovector potential, and $N-Z$ is the neutron excess. Similar equations hold for the corresponding imaginary potentials. Assuming a constant value of $V_1=100$ MeV, we obtain $V_0=51.3$ MeV such that $V^{>}=V_n=47-0.3E_n$. The value of β_n calculated using this potential was shown plotted in Fig. 3. For the proton potential, which we have assumed equal to $V^{<}$, we obtain $V_p=55.6-0.3E_p$. We use this potential to calculate β_p.

We use our empirical value of α_n used in fitting the ^{140}Ce neutron total cross sections together with Camarda's imaginary potential to determine an effective path length for absorption inside the nucleus, i.e., $\bar{R}$ from Eq. (6). The value of $\bar{R}$ is only about 60% of the nuclear radius which is quite consistent with the Camarda *et al.*[7] use of an imaginary potential peaked at the nuclear surface. We then assume $W_1=50$ MeV and finally obtain $\alpha_p=0.08$. Note the values of V_1 and W_1 used here are essentially equal to the Becchetti-Greenlees values.[13]

The results are shown in Fig. 4 where we have plotted the quantity $[\sigma_{is}/2\pi(R+\lambda\!\!\!^{-})^2]$ versus $\sqrt{E_n}$. It is easy to qualitatively understand these results. For $V_1=0$ we

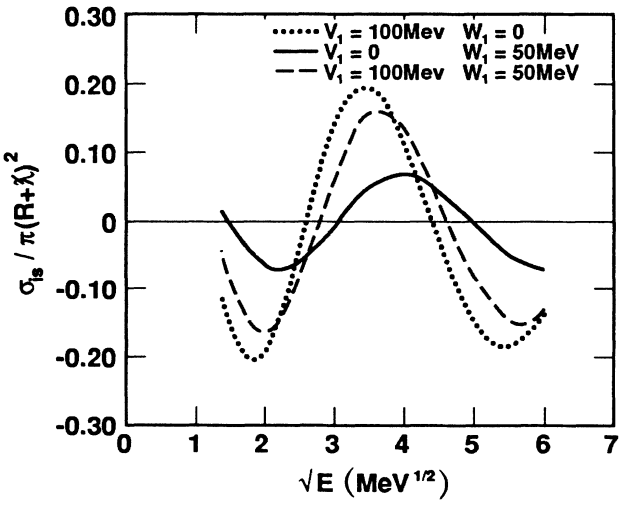

FIG. 4. Twice the normalized isospin transfer cross sections, $\sigma_{is}/\pi(R+\lambda\!\!\!^{-})^2$, is plotted as a function of the square root of the bombarding energy (in MeV). The dotted curve is for $V_1=100$ MeV and $W_1=0$, the solid curve is for $V_1=0$ and $W_1=50$ MeV, and the dashed curve is for $V_1=100$ MeV and $W_1=50$ MeV.

simply have two total cross sections with the same periodic behavior ($\beta_n=\beta_p$) but with different amplitudes subtracted from each other. For $W_1=0$, we have total cross sections of the same amplitude ($\alpha_n=\alpha_p$) but with a phase difference, due to V_1, subtracted from each other. The magnitude of the total cross-section differences are large, reaching values close to a barn at $\sqrt{E_n}=1.8$ and 3.0 MeV$^{1/2}$. Even though these differences are large, the constructing of a nuclear total cross section sans Coulomb from proton scattering data may require significant corrections which will obscure the interpretation of the data and hence the extraction of new information on the isovector potential. Data sets for energy-dependent proton scattering cross sections do not appear to be adequate to warrant further comparisons at this time.

V. PRECISION NEUTRON CROSS SECTIONS FOR ISOTOPIC TARGETS

Since one of our motives for extending the Ramsauer model to include isospin was in looking for sensitivity to the real and imaginary components of the isovector potential, we now explore the sensitivity of total neutron cross sections to the isovector potential. If we go back to our original neutron total cross-section equation (4) and differentiate with respect to a change in neutron number we obtain

$$\frac{\sigma_T^{N+1_T}-\sigma_T^N}{2\pi(R+\lambda\!\!\!^{-})^2}=\frac{2dR}{R+\lambda\!\!\!^{-}}(1-\alpha\cos\beta)-d\alpha\cos\beta+\alpha d\beta\sin\beta\ . \tag{11}$$

We again have an expression where the second and third terms on the right-hand side have different periodic dependences on β and we have the additional first term which just has an A dependence. The derivatives of α and β are now more complicated in that they now have a contribution due to the change in A as well as a contribution due to the change in N, which for a fixed Z, gives us our isospin dependent term. Using Eq. (5) for β, assuming the index of refraction is relatively constant, and including only V_1 in addition to the real central potential V_0, we obtain approximately

$$d\beta=\frac{dN}{3A}\beta\left[1-3/8\frac{V_1}{(\sqrt{V_0+E})(\sqrt{V_0+E}-\sqrt{E})}\right]. \tag{12}$$

The first term is from the change in A due to the addition of a neutron and the second term is due to our change in $(N-Z)$. For V_1 of the order of 100 MeV, the second term is roughly unity in our energy region, so isotopic cross sections, i.e., differences between ^{140}Ce and ^{142}Ce, have little sensitivity to the real part of the isovector potential. Although this result is extremely discouraging, it is equally obvious that if we fix N, e.g., the $N=82$ isotone, and can vary Z, and hence A, by one unit, these two terms which almost canceled will now be additive and the change due to the real isovector potential should be comparable to that caused by our change in radius due to the change in A. Fortunately Camarda *et al.*[7] precisely measured the isotopes we need for such a comparison, i.e., ^{139}La$-^{140}$Ce and ^{141}Pr$-^{140}$Ce.

Rather than fitting the measured total cross sections, we will calculate the various contributions using our simple model and try to obtain a qualitative understanding of the importance of the various terms. First we more precisely define the coefficient in Eq. (11):

$$d\beta=\frac{\beta\delta A}{3A}\left\{1-\frac{3}{8}\frac{V_1}{(\sqrt{V_0+E})(\sqrt{V_0+E}-\sqrt{E})}\frac{\delta(N-Z)}{\delta A}\left[1-\frac{N-Z}{A}\frac{\delta A}{\delta(N-Z)}\right]\right\},$$
$$d\alpha=-\frac{\alpha\ln\alpha}{3A}\delta A\left\{1-\frac{3}{8}\frac{W_1}{W_0\left[1-\frac{N-Z}{8A}\frac{W_1}{W_0}\right]}\frac{\delta(N-Z)}{\delta A}\left[1-\frac{N-Z}{A}\frac{\delta A}{\delta(N-Z)}\right]\right\}, \tag{13}$$

where we have assumed $R=r_0A^{1/3}$. This leads to a change in cross section due to the radius change given by

$$\frac{d\sigma}{2\pi(R+\lambda\!\!\!^{-})^2}=\frac{\delta A}{3A}\left[\frac{2R}{(R+\lambda\!\!\!^{-})}(1-\alpha\cos\beta)+\alpha\beta\sin\beta+\alpha\ln\alpha\cos\beta\right]. \tag{14}$$

We plot this expression in Fig. 5 as well as each of its components. Since β in our energy regime is much larger than $\ln\alpha$, there is little sensitivity to the $\cos\beta$ term.

In Fig. 6 we have plotted the measured total cross-section difference for ^{140}Ce$-^{139}$La versus the square root of the neutron bombarding energy. Also shown as a dot-line is our calculation with reasonably standard parameters, i.e., $V_1=100$ MeV, $V_0=51.3$ MeV, $W_1=14$ MeV. We see the agreement is quite poor. We repeat the calculation increasing the real part of the isovector potential by 50% and increasing the effective change in radius by 50%. Doubling the imaginary isovector potential changes the phase by only a few degrees and produces a slightly worse fit and is not shown. The 50% increase in the change in radius produces a very reasonable fit over the whole energy region except around 6 MeV. We will return to this point later. Increasing the real isovector potential by 50% produces a significant discrepancy around 9 MeV. However, if we shift the calculated curve by 10 mb (compared to an absolute uncertainty in the data of 8

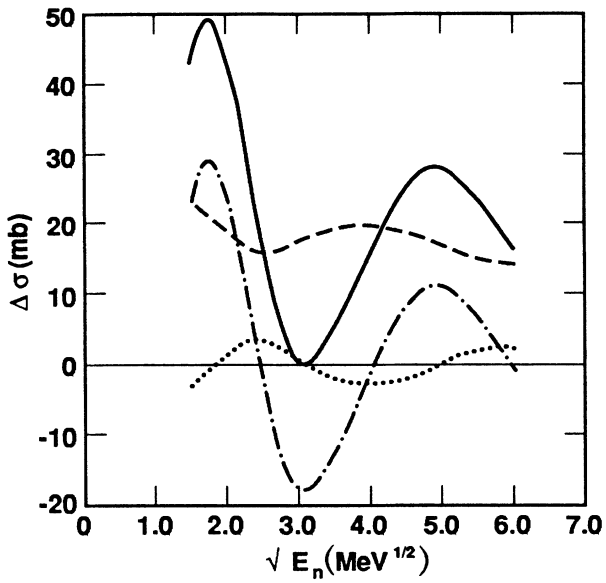

FIG. 5. The difference in total neutron cross sections for adjacent isotopes ($A \rightarrow A+1$) due to a radius change proportional to $A^{1/3}$ is plotted versus the square root of the bombarding energy (in MeV). The dashed curve corresponds to the first term in Eq. (11), the dot-dashed curve is the periodic term proportional to $\sin\beta$, the dotted curve is proportional to $\cos\beta$, and the solid curve is the sum of the three components.

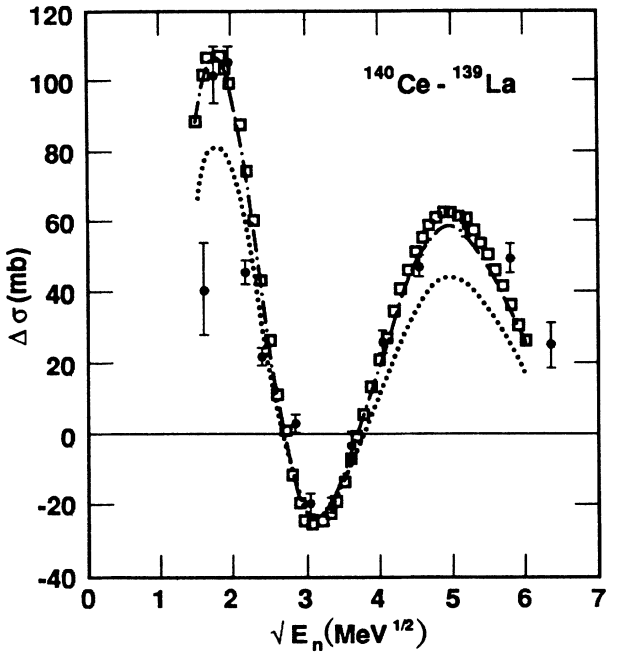

FIG. 6. The difference in total neutron cross sections for $^{140}Ce-^{139}La$ is plotted versus the square root of bombarding energy (in MeV). The dotted curve is calculated for standard parameters. The dot-dashed curve corresponds to a change in radius increased by 50%. The square boxes correspond to an increase in the real isovector potential by 50% and an absolute displacement adjustment of 10 mb. The data are from Ref. 7.

mb), we find that it produces an adequate fit to the data. From other considerations[7] the 50% increase in radial change is quite reasonable but the absolute uncertainties in the data would allow V_1 values ranging from 100 to 150 MeV if there were no external constraints on the radial change.

In Fig. 7 we have plotted the $^{141}Pr-^{140}Ce$ total cross-section difference shifted lower by 15 mb. The fact that the unshifted data did not go below zero at about 9 MeV would have implied that the real part of the isovector potential is zero. On the other hand, with this displacement of the data by 15 mb (compared to an absolute uncertainty in the data of ~ 8 mb), we obtain fair agreement with our best fit curve from Fig. 6. This also comes close to satisfying the requirement that the two curves should be identical.

In Fig. 8 we show the comparison on the $^{142}Ce-^{140}Ce$ difference with this model. As we noted when discussing Eq. (12), the isovector terms, real and imaginary, tend to cancel the $\sin\beta$ and $\cos\beta$ terms from the radius change. Therefore, the average cross-section difference is sensitive only to the first term in Eq. (11) and effectively determines the radius change as ~ 1.5 times that of a liquid drop. The shape, however, is obviously incorrect. It is quite clear that, in order to fit the data, we need to reverse the sign of W_1 and increase its magnitude by a factor of 5. At this point it should be clear that our assumption that W_0 is constant over these isotopes is not correct and what we are observing is a variation in W_0 in going from ^{140}Ce to ^{142}Ce which is large compared to our imaginary isovector potential. This same effect is also visible as a difference between the $^{139}La-^{140}Ce$ and $^{141}Pr-^{140}Ce$

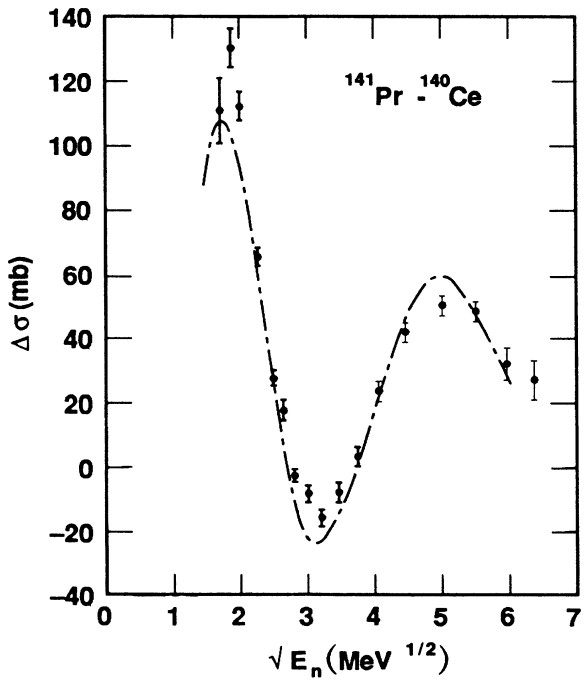

FIG. 7. Same as Fig. 6 for $^{141}Pr-^{140}Ce$. The data from Ref. 7 have been displaced by minus 15 mb.

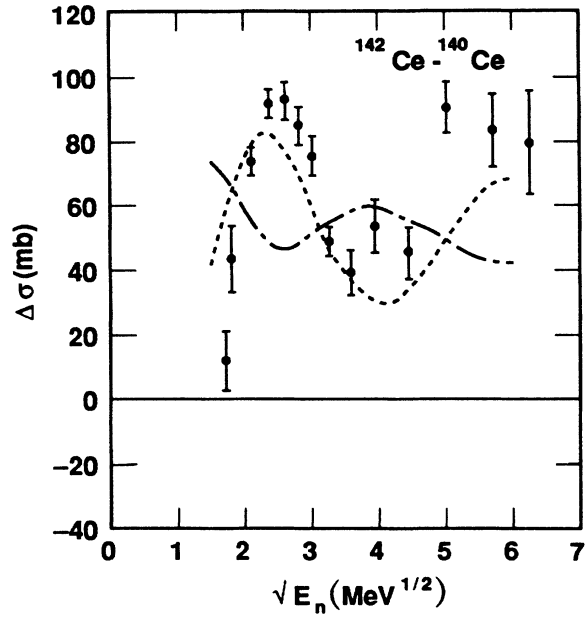

FIG. 8. Same as Fig. 6 for $^{142}Ce-^{140}Ce$. The dot-dashed curve corresponds to a 50% increase in the radius change. The dotted curve corresponds to a change in the imaginary potential five times as large as our standard isovector imaginary potential and of the opposite sign. The data are from Ref. 7.

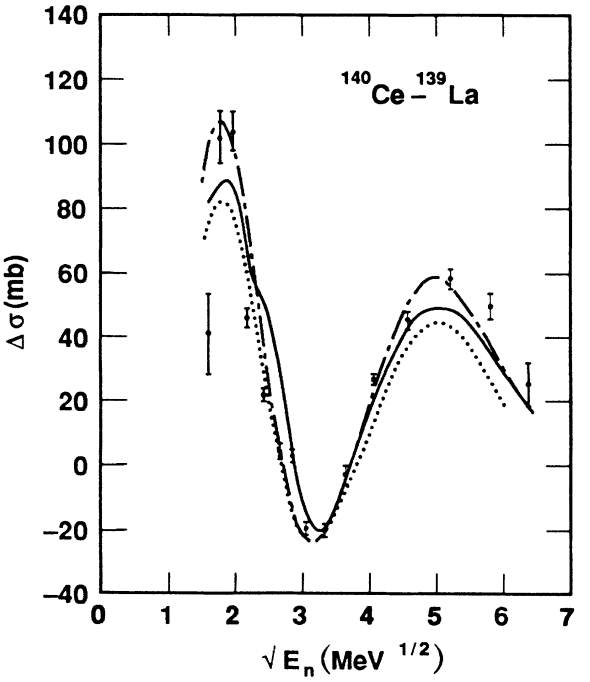

FIG. 9. Same as Fig. 7. The solid curve is the optical-model calculation from Ref. 7, Fig. 7 (solid curve).

curves around 6 MeV. The measured difference is opposite from what would be caused by a reasonable W_1 and is compatible with the level structure of the La and Pr isotopes. The changes in radii required by our model are very similar to those extracted by Camarda *et al.*[7] in their optical-model analysis of these data. In Fig. 9 we show the optical calculations for the $^{140}Ce-^{139}La$ total neutron cross-section differences compared to our simple model. The most significant difference between the optical calculations and our simple model is in the 6–8-MeV energy region. This is largely accounted for by the almost factor of 2 larger imaginary isovector potential used in the optical-model calculations. Note this larger potential produces poorer agreement with the data and also indicates the sign of the imaginary potential change needed to fit the data is opposite of that associated with the isovector potential.

For the real central and isovector potentials, which have volume Woods-Saxon form factors, it seems plausible to compare optical calculations with our Ramsauer model using the same parameters. From Fig. 3, where we used $n=1.32$ in Eq. 5, we see that our empirically determined β differs from the values using optical-model parameters only below 9 MeV ($\sqrt{E}=3$ MeV$^{1/2}$). In Fig. 9 this would move our calculated lowest-energy maximum from $\sqrt{E}=1.8$ to 1.5 MeV$^{1/2}$ with the position of subsequent maximum and minimum above $\sqrt{E}=3$ MeV$^{1/2}$ remaining unchanged. Using the same isovector potential as for the solid curve, the extremes in the oscillations in the dotted curve would be reduced by about 10%. No similar argument for a simple correspondence between parameters can be made for the imaginary potential because it varies from a pure surface peaked form factor at low energies to a pure volume form factor at high energies. We conclude that although our model may give semiquantitative agreement with some aspects of the data, optical-model calculations should be used for quantitative comparisons.

VI. CONCLUSIONS

The simple Ramsauer model fits the ^{140}Ce total cross-section data quite well. In the neutron energy range of 3–30 MeV the model reproduces the measured data with a relative precision of $\sim 1\%$ and within the absolute quoted accuracy of 1.5–2%. Previous applications of this model have produced semiqualitative agreement with data. Our agreement is far better than anticipated, given that we have used only four free parameters.

Having fit the precision total cross-section data, we extended the model to include isospin. The anticipated phase sensitivity of the isospin transfer cross section was demonstrated for small values of the isovector potential. However, for realistic isospin potentials ($V_1 \sim$ 100 MeV and $W_1 \sim 50$ MeV), even though the predicted cross-section difference was almost 2 orders of magnitude greater than the corresponding spin-spin case, there appears to be little sensitivity to the imaginary part of the isovector potential. This coupled with the uncertainties introduced when we include the Coulomb potential renders this line of research as speculative.

Using this same approach to analyze precision isotopic total cross sections, we obtain a value for the real isovector potential which is consistent with other measurements. However, the dominant effect observed is due to changes in the nuclear radius and changes in the isoscalar imaginary potential around the shell closure at $N=82$. Both of these effects should be less important for data measured on neighboring isotopes farther from closed shells. Although difficult to perform, these measurements would be quite useful.

A seemingly surprising result, which is obvious in the present analysis but is also found in the earlier analysis,[7] is the large change in W_0 between neighboring isotopes at a bombarding energy of 9 MeV. This is an energy at which most global analyses have reached their asymptotic region and show minimum shell effects. However, the analysis of Grimes,[14] which involved microscopic calculation of 2p-1h states, found significant shell effects persisting at energies as high as 6 MeV. Extrapolation of these results to higher energies seems to be consistent with our current results.

This means we can examine changes in W_0 by analyzing cross-section differences near closed shells, and that to extract imaginary isovector strengths, we must stay far from closed shells.

Two other conclusions follow from the simple analysis here. As has been pointed out by McVoy, Ramsauer modulations are due almost entirely to energy variations in the elastic scattering cross section. Much smaller modulations in the absorption cross section are attributed to single-particle resonances, rather than the echoes (passing through $\pi/2$ in the negative direction) which cause the Ramsauer peaks. From this, it seems immediately clear that analyses of elastic scattering on adjacent isotopes will show minimal sensitivity to V_1, because the changes in elastic scattering caused by V_1 and those produced by variations in R will tend to cancel. On the other hand, corresponding analyses for proton elastic scattering should show enhanced sensitivity, but will require the changes in radius to be well determined (by electron scattering, for example) before unambiguous results for V_1 can emerge. Comparison of the neutron elastic cross sections for isotones (equal N) would show enhanced sensitivity to V_1 and the corresponding cross sections for protons reduced sensitivity, again because of cancellation effects.

The present analysis confirms the conclusions reached by Camarda *et al.*[7] Considerable information about the optical model is available from neutron total cross sections. Use of simple Ramsauer based analysis can help identify limits on sensitivity, reactions, and energy regions.

This work was performed under the auspices of the U.S. Department of Energy by the Lawrence Livermore National Laboratory under Contract No. W-7405-ENG-48.

---

*Permanent address: Department of Physics, Ohio University, Athens, OH 45701.

[1]J. D. Lawson, Philos. Mag. **44**, 102 (1953).

[2]A. Bohr and B. Mottelson, *Nuclear Structure* (Benjamin, New York, 1969), Vol. 1, p. 166.

[3]J. M. Peterson, Phys. Rev. **125**, 955 (1962).

[4]K. W. McVoy, Ann. Phys. (N.Y.) **43**, 91 (1967).

[5]Leonard I. Schiff, *Quantum Mechanics* (McGraw-Hill, New York, 1949), p. 109.

[6]C. R. Gould, D. G. Haase, L. W. Seagondollar, J. P. Soderstrum, K. E. Nash, M. B. Schneider, and N. R. Roberson, Phys. Rev. Lett. **57**, 2371 (1986).

[7]H. S. Camarda, T. W. Phillips, and R.M. White, Phys. Rev. C **29**, 2106 (1984).

[8]K. W. McVoy, Phys. Lett. **17**, 42 (1965).

[9]One would prefer a quadratic least-squares fit but this form does not give a good fit to the data. For the same number of parameters the two linear curves produce a significantly better fit to the data.

[10]M. A. Nagarajan, C. C. Mahaux, and G. R. Satchler, Phys. Rev. Lett. **54**, 1136 (1985); C. Mahaux and R. Sartor, *ibid.* **57**, 3015 (1986).

[11]We shall see later this assumption is not justified. See Fig. 4.

[12]A. M. Lane, Phys. Rev. Lett. **8**, 171 (1962).

[13]F. D. Becchetti and G. W. Greenlees, Phys. Rev. **182**, 1190 (1969).

[14]S. M. Grimes, Phys. Rev. C **22**, 436 (1980).